UNIVERSITY OF CALIFORNIA SAN DIEGO

Simulating Vacancy Formation and Diffusion in NbMoTaW

A thesis submitted in partial satisfaction of the requirements for the degree Master of Science

in

Materials Science and Engineering

by

Luke Nibbelink

Committee in charge:

Professor Shyue Ping Ong, Chair
Professor Marc Meyers, Co-Chair
Professor Vitali Nesterenko

The thesis of Luke Nibbelink is approved, and it is acceptable in quality and form for publication on microfilm and electronically:

Co-Chair

Chair

University of California San Diego

2020

Table of Contents

Signature Page iii

Table of Contents iv

List of Figures v

List of Tables vi

Acknowledgements vii

Abstract of the Thesis viii

Introduction 1

HEAs 1

Simulations 3

Defects 9

Motivation and Proposed Study 15

Chapter 1: Vacancy Formation Energy (VFE) Calculations 16

Chapter 2: Calculating Migration Enthalpy in NbMoTaW 22

Chapter 3: Conclusion and Future Work 35

References 37

List of Figures

Figure 1: Standard Neural Net (a) and Scalable Neural Net for Interactions at the atomic level (b) 7

Figure 2: VFE for different species being replaced for a vacancy 10

Figure 3: Regular lattice site on the left-hand side, trapping lattice site on the right-hand side... 12

Figure 4: Computed Vacancy Formation Energies from SQS Structure in LAMMPS 18

Figure 5: Computed Vacancy Formation Energies of the Five Lowest VFEs from DFT and LAMMPS for each Specie 19

Figure 6: Profile View of Diffusion Bottleneck (a) and Top-Down View of Diffusion Path Bottleneck (b)..... 27

Figure 7: Bar Graph for Migration Enthalpies for Nb-W Alloy for all Bottleneck Configurations and Three Matrices (denoted in different colors) 29

Figure 8: Profile View of 1NN Core (a) and Top-Down View of 1NN Core (b)..... 30

Figure 9: Graph of Relaxed Cell Migration Enthalpies with Different Core Sizes 33

Figure 10: Graph of Relaxed Cell Migration Enthalpies with Different Core Sizes 33

List of Tables

Table 1: The VFE Averages and Standard Deviations for each Specie when Using Each Simulation Software……...…19

Table 2: VFEs for Constituent Species from NbTaMoW in their Pure Form.....20

Table 3: Migration Enthalpies for Constituent Elements of NbMoTaW…….....25

Table 4: Migration Enthalpies for Nb-W Alloy for all Bottleneck Configurations and Three Matrices……..28

Table 5: Relaxed Cell Migration Enthalpy [eV] Calculations with Different Core Sizes…...….32

Table 6: Fixed Cell Migration Enthalpy [eV] Calculations with Different Core Sizes…….…....32

Acknowledgements

I am incredibly thankful for the help and assistance I received to create this thesis. First, I would like to thank Dr. Shyue Ping Ong for allowing me to work in his group and do this research. In addition to the consistent and imperative guidance he provided throughout my research, he provided me with the computational resources and processing scripts necessary to perform the work. I also want to thank Dr. Marc Meyers for introducing me to Dr. Ong and for sitting on my committee. I would like to thank Dr. Vitali Nesterenko for also sitting on my committee.

I am also thankful to Hui Zheng for with helping me perform my research. She graciously helped me work through the numerous questions I had throughout my research and taught me how to perform many of the necessary calculations. Xiang-Guo Li also helped me structure my experiments and taught me how to perform calculations. I would also like to thank Mahdi Amachra for teaching me how to work with the supercomputing clusters.

Finally, I am thankful to my parents for their continued support in my endeavors. They have been with me through thick and thin, and I will forever be grateful.

ABSTRACT OF THE THESIS

Simulating Vacancy Formation and Diffusion in NbMoTaW

by

Luke Nibbelink

Master of Materials Science and Engineering

University of California San Diego, 2020

Professor Shyue Ping Ong, Chair

Professor Marc Andre Meyers, Co-Chair

High entropy alloys (HEAs) demonstrate remarkable properties which are useful in critical engineering applications. Recent studies report that NbMoTaW exhibits many of the properties similar to HEAs, including high hardness, high electrical resistance, and high thermal

stability. In turn, selecting and implementing the NbMoTaW alloy would improve components in power and nuclear applications. This Master's thesis will discuss vacancy formation and diffusion behavior in NbMoTaW, along with atomistic simulations that can capture that phenomena. DFT and MD simulations as implemented in VASP and LAMMPS, respectively, calculated vacancy formation energies for the NbMoTaW HEA using an SQS structure. These vacancy formation energy calculations show that Nb and Ta vacancies are the most energetically favorable and illustrate some discrepancies between the MD and DFT simulations. In addition, DFT simulations used the climbing image NEB method as implemented in VASP calculated migration enthalpies in the Nb-W alloy. These calculations used a set of structures which have different atomic compositions in the local environment. The composition changes in the set of structures surrounded the diffusion path and varied in the spatial distance from the diffusing atom. DFT simulations using the climbing-image NEB method as implemented in VASP showed that a change in composition five nearest neighbors away from the diffusion path had a non-negligible effect on the migration enthalpy, however the error peaked at three nearest neighbors.

Introduction

HEAs

HEAs, also called Multi-Principal Element alloys, are a solid solution of multiple alloying elements. In general, each alloying element encompasses a nearly equivalent composition of the overall material. HEAs exhibit exceptional properties that match or exceed the capabilities of state-of-the-art superalloys. HEAs differentiate themselves with superior hardness, strength, electric resistance, and stability at high temperatures. For example, a recent study reported a peak hardness of $\sim 16.0\ GPa$ and a high electrical resistance of $\sim 170 \mu\Omega * \text{cm}$ for the NbMoTaW refractory HEA [1]. In theory, the outstanding properties observed in HEAs are due to lattice distortion and the variety of alloying elements distributed randomly through the system to prevent atoms from diffusing. This path of reasoning led to the name 'High Entropy Alloy,' as the random distribution in a variety of atoms increases the disorder, or entropy, in the system. This disorder can stabilize the material structure by balancing the mixing entropy and mixing enthalpy contributions, as shown in the Gibbs free energy equation (Equation 1), to improve phase stability [2].

$$\Delta G = \Delta H - T\Delta S \qquad \text{Equation 1}$$

This theoretical understanding is not always consistent, so a considerable amount of research investigates other contributions to behavior in HEAs [3].

Examining the microstructure of HEAs yielded additional reasons why strengthening occurs in HEAs. A face centered cubic (FCC) HEA, $Co_{25}Ni_{25}Fe_{25}Al_{7.5}Cu_{17.5}$, manufactured utilizing mechanical alloying (MA) followed by spark plasma sintering (SPS), was analyzed

utilizing X-ray diffraction (XRD) and transmission electron microscopy (TEM). The analysis found average grain sizes of 95 nm after SPS and a high concentration of twins. The compressive yield strength was significantly higher than other manufactured HEAs [4]. The electrical resistance was not as dependent on the thickness of the thin film relative to other alloys and the study attributed this characteristic primarily to the considerable lattice distortion in the HEA.

Researchers manufactured a body centered cubic (BCC) HEA, NbMoTaW, on thin films using current magnetron sputtering. This alloy demonstrated high thermal stability, hardness, and electric resistivity. The study reporting on the researchers work demonstrated high thermal stability by heating the alloy to 800°C for two hours and seeing the grain size grow from 8.6 to 9.5 nm. Further analysis attributed the relatively slow grain growth to slow, or 'sluggish,' diffusion [1]. The study attributed the high hardness of this alloy to the small grain size and that the material was deposited as a thin film [5]. Another study demonstrated that the electrical resistance in NbMoTaW was not as dependent on the thickness of the thin film and instead was attributed primarily to the considerable lattice distortion in the HEA [1].

Lattice distortion is an inherent and impactful factor for HEAs. The different atomic sizes in the alloying elements cause the lattice distortion in the system, extending and impeding possible diffusion paths. Lattice distortion results from the mixing of different alloying elements with dissimilar atomic sizes forcing the lattice to distort from a simple repeating crystal system, often cubic, to lose any resemblance of short or long range order [6]. Most of the literature on HEAs up to the time of writing of this paper has focused on FCC transition metals. These transition metal HEAs have garnered attention for their improved fracture toughness and strength at cryogenic temperatures compared to their alloying elements in a pure form. Recent research

reports HEAs alloyed with BCC refractory elements, like the HEA NbMoTaW, have high strength and thermal stability [3].

Simulations

Producing HEAs in bulk has not been achieved yet, preventing experimental tests on large quantities of the alloy. It is difficult to adequately mix the alloying elements to form a proper HEA and avoid creating unintentional, heterogeneous phases within the material. There have been experimental tests on smaller samples of HEAs, which provided data on defect formation and motion. These tests are currently limited to small sample sizes and thin films [7]. The inability to create a large sample of an HEA is a bottleneck for gathering a variety of information on HEAs. To overcome this, researchers use simulations of HEAs extensively. Simulations offer a wider range of samples and more control over a test. Due to the random nature of HEAs, no configuration of atoms will be the same between one sample and another. Therefore, researchers must test many different configurations to accurately predict a HEA's behavior. Simulations allow the researcher to control the atomic structure's configuration during tests and to perform more of those tests. Highly accurate simulations tend to be computationally expensive and vice versa, so each study must strike a compromise.

The unique atomic structure of HEAs require small scale simulations to determine the characteristics that produce preferred properties. The two types of tests that are sufficient are density functional theory (DFT) and molecular dynamics (MD) simulations. DFT utilizes theorems proved by Kohn and Hohenberg which stipulate that '*the ground-state energy from Schrödinger's is a unique functional of the electron density*', and that '*the electron density that minimizes the energy of the overall functional is the true electron density corresponding to the*

full solution of the Schrödinger equation' [8]. In essence, DFT utilizes equations which describe the electron density of a material and finds the spatial configuration and atomic interactions that minimize the overall energy, or ground-state energy, of the system. In theory DFT can perfectly simulate any material, however calculations make approximations as the computational cost would be insurmountable. The Vienna Ab initio Simulation Package (VASP) is used for most HEA simulations using DFT, which implements the generalized-gradient approximation (GGA) using the Perdew-Burke-Ernzerhof (PBE) exchange correlation functional [3]. MD simulations utilize empirical atomic potentials to simulate materials. MD simulations are orders of magnitude faster than DFT simulations, however their accuracy is limited by the empirical potential they are based on [3]. If the empirical potential is not capable of simulating complex magnetic interactions between atoms or a unique combination of atoms are simulated that had not been thoroughly studied yet, then the simulation could be too inaccurate to be useful. Large-scale Atomic/Molecular Massively Parallel Simulator (LAMMPS), developed by Sandia Labs, is most often used with MD.

HEAs are inherently difficult to simulate, as their atomic configuration is randomly distributed. Each lattice site will have a different local environment because the atoms surrounding that site are different species and take varying positions from lattice distortion. As a result, the computational cost of running enough tests to be confident in the results are daunting. Studies with sufficient statistical power require either a single 10^4 atom simulation or 10^6 small and dissimilar simulations [3]. Therefore, researchers can use different strategic approximations to overcome this computational hurdle.

Some studies have used the coherent potential approximation (CPA) implemented with exact muffin-orbitals (EMTO) if local effects do not influence the property being calculated.

This method utilizes the mean field approach to approximate the random spatial distribution of atoms as an average [9]. In HEAs, this manifests as calculating the average occupation of lattice sites by each type of specie and assuming that the local potential around the same type of atom are identical. Using CPA with EMTO is drastically cheaper to compute relative to most other simulation methods. Overall, it can also be incredibly accurate calculating general properties of a material like lattice parameter and Young's modulus or describe the energetics for point and linear defects. However, when the structure is no longer at a ground state, local distortions have more of an influence, and other simulations must be used [3].

Another strategy is to use a special atomic structure that includes as many unique and pertinent atomic interactions present in an actual HEA as possible. Special quazi-random structures (SQS) rely on pairing and multiscale functions that correlate spatial characteristics from a large set of fully disordered HEA structures. Using the pairing and multiscale functions one SQS structure is constructed that includes all the characteristics from the set of HEA structures [3]. Researchers have used SQS structures for a wide range of calculations involving HEAs in many ways. A recent study calculated appropriate lattice constants and determined the influences nanotwins had on the strengthening mechanisms in FCC HEAs [10].

At times, one SQS structure is not sufficient. Identifying one structure that represents a specific HEA adequately is a challenge as more alloying elements are added. To have a structure that will include all the sufficient atomic interactions, the cell size will become too large to model. In addition, the number of correlation functions will go out of control, preventing even generating the structure to begin with. A possible solution to this is using a small set of ordered structures (SSOS), where the researchers tailor a set of structures to reflect the atomic phenomena studied is modeled and can reduce the computational cost [3]. A study on the phase

stability of the BCC refractory HEA VNbMoTaW at different compositions and temperatures used multiple ordered and SQS structures. This study reported a temperature range where each SQS structure was stable. Each structure has a unique composition and atomic structure, and so using multiple representative structures was computationally cheaper than using one massive SQS structure to represent the entire HEA [11].

MD simulations require orders of magnitude less computational resources compared to DFT simulations; however, MD models do not capture many of the complexities DFT is able to. MD simulations rely on existing interatomic potentials, which usually are not created with the capability to model alloyed metals. Researchers have simply combined binary and ternary interatomic potentials to simulate HEAs as these potentials will simulate most of the interactions in the material [3]. Another type of potential has been developed to address this challenge, second nearest-neighbor modified embedded-atom method (2NN MEAM). This method constructs an interatomic potential which utilizes parameters that have been published for unary and binary alloys, and then calculates more parameters for the unknown interactions from analytical mechanics. 2NN MEAM has been used to simulate HEAs, largely when unary, binary, and ternary interatomic potentials are already available for the alloy's constituent elements. In a study concerning the CoCrFeMnNi HEA, 2NN MEAM was used in a study that simulated equilibrium structure and the effect alloying had on the critical resolve shear stress (CRSS), which was validated experimentally [12].

Machine learning (ML) approaches are also used in developing interatomic potentials. The ML algorithms use a descriptor for the symmetry of the material and has a covariate to act as a regressor that models the potential. The descriptor must use characteristics that are consistent between the atomic and electronic structure. These would be something like lattice parameters,

space groups, or an atomic species' electronegativity [3]. Artificial neural networks (ANN) allow for describing complex, nonlinear correlations between a material and its behavior. ANNs are models that adjust weights associated with nodes in a layered neural net, which allows for a considerable amount of flexibility. However, scalability can be challenging as the input nodes include all the atoms in the system, each atom in the system could increase the computational cost of the model exponentially. By constructing a neural net that describes interactions at the atomic level rather than the entire structure, which is dependent on the number of atoms in the model, the complexity of the model can be reduced [13]. As seen in Figure 1, the algorithm adjusts weight parameters (w_{ab}^{c}) each time the input layer. Or atomic structure, is changed in the standard neural net for ML produced interatomic potentials. The scalable neural net as seen in Figure 1, adds an additional layer for the Cartesian coordinates of the atoms in the system $\{R_b^a\}$ before calculating symmetry function values $\{G_b^\mu\}$ so that scalability is built into the model [13]. This new model was tested on silicon to predict the phase at different temperatures. Using 8200 DFT calculations for training the model and 800 more for testing, the model performed significantly better than previously published neural networks.

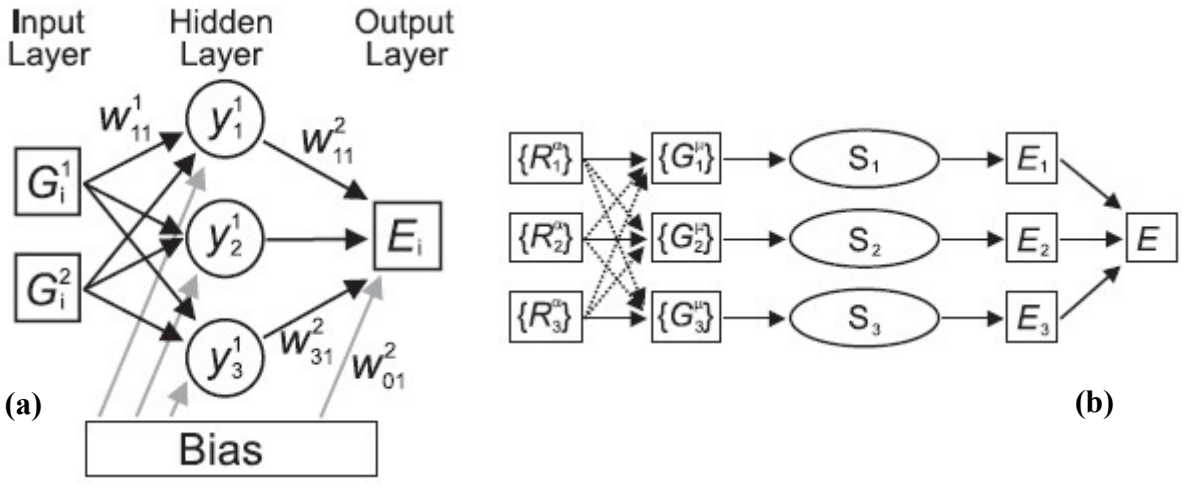

Figure 1: Standard Neural Net (a) and Scalable Neural Net for Interactions at the atomic level (b) [13]

Gaussian approximation potential (GAP) and spectral neighbor analysis potential (SNAP) are common ML frameworks for interatomic potential development. Both utilize local neighbor density as a descriptor, and they differ in that GAP uses Gaussian regression and SNAP uses least-squared linear regression. These methods tend to be an order of magnitude more expensive relative to using already-developed interatomic potentials, however they are orders of magnitude faster than just using DFT simulations [3]. These approximations can be incredibly useful when simulating complex interactions in HEAs that need a larger set of atoms. Classic potentials often cannot simulate the complex interactions of multiple transition metals in one alloy and simulating atomic behavior with more than a few hundred atoms in DFT is largely infeasible due to computational cost. A recent study on the refractory BCC HEA NbMoTaW utilized SNAP to create an interatomic potential that was able to simulate cell sizes that reached into the tens of thousands of atoms. With these large supercells larger scale behavior could be observed. NbMoTaW showed a tendency for Nb segregation to grain boundaries (GB), comparable strengths for screw and edge dislocations, and specific species-rich regions with predictable high or low von Mises strains. These insights will help inform researchers about the material whether they are manufacturing or using it [14].

Force field methods, which instead of using the potential energy field skips directly to atomic interactions, are also used. These models use Atomic forces as descriptors which also incorporates the local environment, and use Beysian inference, kernel ridge regression, and Gaussian process regression as regressors [3].

Defects

The subject of interest for most simulations are defects. Defects, as in all materials, have a considerable influence on behavior in HEAs. Point defects, vacancies and self-interstitials in particular, incentivize research in HEAs as they tend to have more of an effect in that class of alloy. More alloying elements in HEAs cause lattice distortion and configurational entropy, which leads to more instances of point defects in HEAs [12]. This distinction contributes to many of the unique properties of HEAs, including diffusion behavior and radiation tolerance [3].

It is challenging to theoretically describe the energetics of vacancies accurately so DFT and MD simulations are incredibly useful in predicting vacancy behavior. A useful calculation is for vacancy formation energy (VFE). VFE, or the energy required to create a vacancy, can govern the phase stability or segregation behavior for an HEA. The equation for calculating VFE is shown in Equation 2, where E_v is the energy of the supercell with the defect, μ_a is the chemical potential, and $E_{pf}$is the energy of the perfect supercell.

$$E_v = E_{df} + \mu_a - E_{pf} \qquad \text{Equation 2}$$

Unstable phases in HEAs can pose challenges for researchers because the alloy can lose some of its efficacy as separate phases form with lower amounts of alloying elements. However, vacancies and all other defects in HEAs are inherently challenging to simulate due to the random nature of the material. Surrounding atoms will affect the conditions of a defect in a HEA, and the total set of possible atomic structures is a combination of the number of alloying elements and the number of sites a study considers [3]. Therefore, researchers usually report VFE as a distribution and report statistics on that distribution. An example of this is a study on the FCC HEA CrCoFeNi that calculated, among other things, many VFEs for different structures and

different species. The study tested different structures with different binding energies and changed the specie of the diffusing atom. Figure 2 displays the VFE results from that study. From this test, the authors were able to recognize that the Cr atoms were unstable in this HEA, as they all had negative VFEs. They were also able to tailor the composition of the alloy to allow the Cr atoms to stabilize [15].

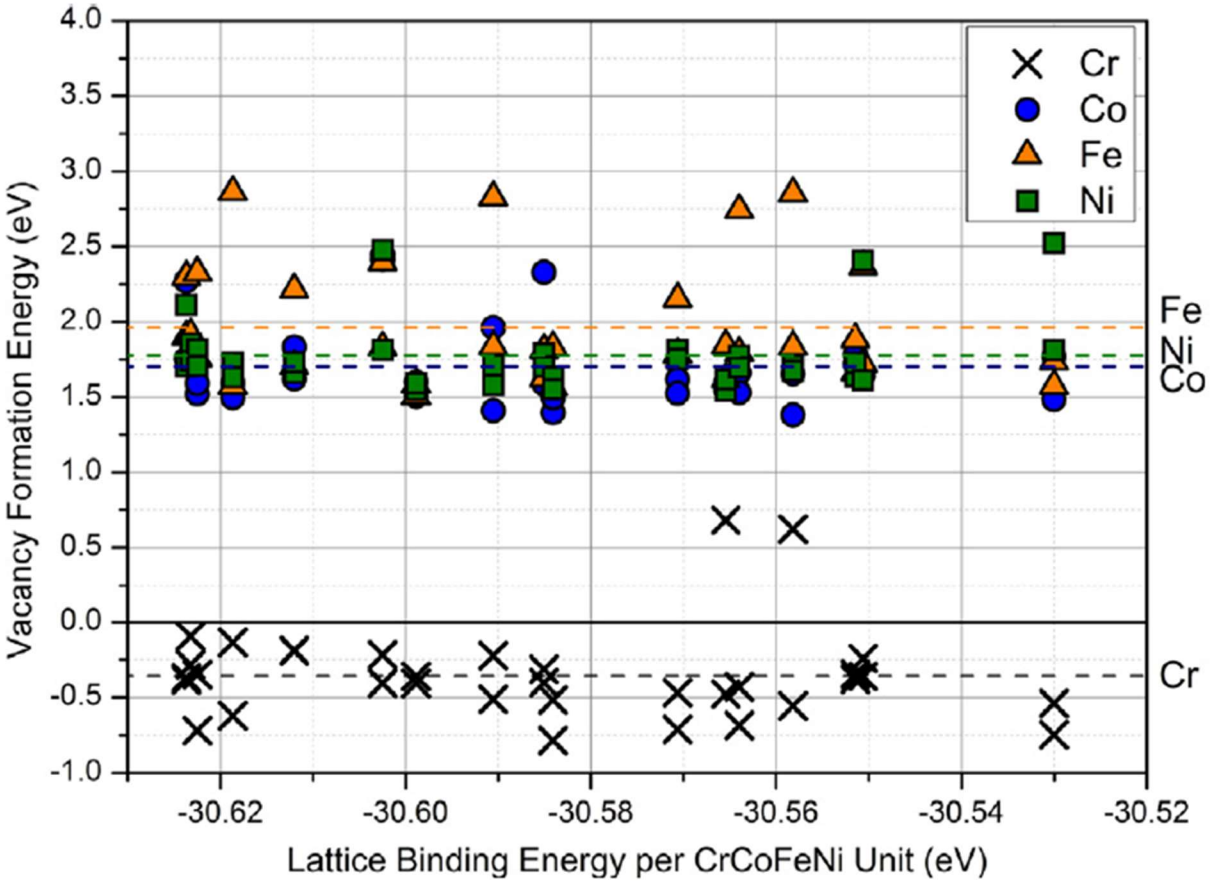

Figure 2: VFE for different species being replaced for a vacancy

[15]

One of the most notable characteristics about HEAs is sluggish diffusion. Sluggish diffusion gives HEAs thermal stability and the ability to retain strength at high temperatures. The reasons why sluggish diffusion occurs in HEAs is still debated. The conventional thinking is that

the more alloying elements in the alloy, the more chemical disorder and lattice distortion there is, the more difficult it is for atoms to move from one place to another. However, recent studies demonstrated that an increase in alloying elements does not necessarily impede diffusion [3]. A study which demonstrated this observed tracer Ni diffusion in CoCrFeNi to be faster than tracer Ni diffusion in CoCrFeMnNi [16]. However, researchers identified characteristics pertaining to the space local to vacancy, like trapping lattice sites, lattice distortion, and interatomic correlations, slows down diffusion in HEAs.

Trapping lattice sites occur when the atoms surrounding a vacancy are all the same species. A distinction between a regular HEA lattice site and a trapping lattice site is shown in Figure 3. In a regular lattice site in an HEA, different atomic species surround a vacancy and the structure has characteristics common to HEAs: high levels of lattice distortion, more atomic disorder, and higher binding energies. A trapping lattice site is energetically favorable because the local lattice exhibits the character of a pure material around the site [17]. Due to the trapping site being favorable to other sites the vacancy can take, the migration barrier for the vacancy increases considerably. Even when the vacancy exits the trapping lattice site, it is very likely to return due to the energetically favorable vacancy site [3].

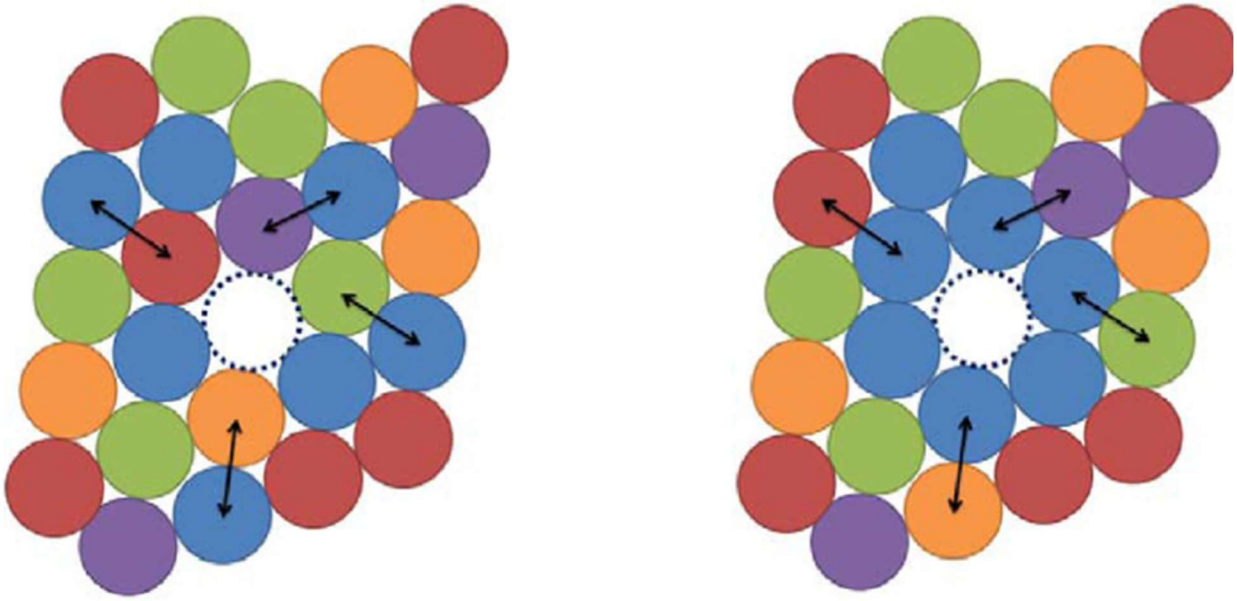

Figure 3: Regular lattice site on the left-hand side, trapping lattice site on the right-hand side [17]

Vacancy diffusion is important as it affects many of the unique characteristics of HEAs, so simulating vacancy diffusion is also important. The most common calculation is the nudged elastic band (NEB) method. When using NEB, diffusion is simulated by calculating the structure's energy as an atom travels along certain positions on a diffusion path. These positions include a start and endpoint, which are identified by the user, in addition to a specified number of positions along the diffusion path, which are called images. The vacancy migration barrier is calculated by taking the difference between the position with the highest energy, called the saddle point, and the mean of the energies of the start and endpoint. Vacancy migration barriers in HEAs vary widely because of the random configuration of atoms that fill the space near the diffusion pathway [3]. Similar to VFEs, studies report vacancy migration barriers as distributions when simulating HEAs due to their random nature. A study was able to inform a Kinetic Monte Carlo simulation with vacancy migration energies calculated with DFT using the NEB method.

The model analyzed the CoNiFeCrMn HEA and identified Mn as having a lower migration barrier relative to the other elements [18].

Self-interstitials are also an important point defect in HEAs. Their formation energies relative to vacancies are relatively high, therefore they form in high energy circumstances like radiation. Calculating self-interstitial formation energies is fairly similar to calculating VFEs, as seen in Equation 3, similarly to Equation 2. In Equation 3, E_i is the formation energy of the self-interstitial, E_{df} is the energy of the defective supercell, μ_a is the chemical energy of the interstitial atom, and E_{pf} is the energy of the perfect supercell [3].

$$E_i = E_{df} - \mu_a - E_{pf} \qquad \text{Equation 3}$$

Self-interstitials, unlike vacancies, require less energy to form in a HEA relative to a pure metal [3]. The study that determined this found that Ni in CoCrFeNi required less energy to form a self-interstitial relative to Ni forming an interstitial in pure Ni. The opposite of that was true for vacancies, where the VFE with Ni being replaced with a vacancy in CoCrFeNi was higher relative to the VFE in pure Ni [19].

Diffusion rates for self-interstitials in HEAs tend to be higher than pure metals. In addition, with the lower formation energy for self-interstitials in HEAs, clusters of these imperfections will form. Clusters of self-interstitials will inhibit diffusion further as more atoms in interstitial sites will block one another. Directional diffusion is also inhibited in HEAs, as the lattice distortion randomizes the diffusion paths available to self-interstitials. This will also reduce the diffusion rate in HEAs as interstitials will exhibit a random walk pattern rather a linear one. Due to the diffusion speed of self-interstitials being slower than that of vacancies and self-interstitials tend to form in clusters, vacancies and interstitial atoms will recombine at a high

frequency. These properties in tandem demonstrate how HEAs have such a high radiation resistance.

Motivation and Proposed Study

Research on HEAs is a worthwhile pursuit, as this new class of alloy has demonstrated exciting capabilities, however limited understanding has been a barrier to scalability and optimization of these alloys. The scale of the composition space of HEAs is massive, so the focus of this study will be on the NbMoTaW alloy. The NbMoTaW alloy has been noted to have a measured peak hardness of $\sim 16.0\ GPa$ and a high electrical resistance of $\sim 170\ \mu\Omega * \text{cm}$ in addition to a high level of thermal stability because after two hours of vacuum annealing at $800°C$ the alloy kept it's BCC structure [1]. To elucidate the mechanisms behind these exceptional properties, there has been research on simulating the NbMoTaW alloy. Another study utilized SNAP to simulate NbMoTaW and investigated dislocation mechanics, Nb segregation, and grain boundary stability due to a reduction in the von Mises strain in the grain boundary [14]. This study was discussed in the Simulations section in the Introduction. This master's thesis intends to add to the current information around the NbMoTaW alloy by utilizing LAMMPS and DFT simulations to describe vacancy diffusion. Vacancies have a considerable effect on the behavior of an HEA, and simulating vacancy behavior in NbMoTaW has had limited focus. In addition, the effects distances have on interatomic interactions will be studied. The challenges associated with the randomness of HEAs mean that many simulations must be performed to consider all the possible atomic configurations. This thesis will simulate the effects of atomic changes at different distances from vacancy diffusion in a Nb-W alloy and compare the migration enthalpies of these simulations.

Chapter 1: Vacancy Formation Energy (VFE) Calculations

As discussed in the Defects section of the Introduction, vacancies have a considerable effect on the behavior in HEAs. Vacancies contribute to diffusion rates, radiation damage resistance, and segregation in the alloy. Vacancies decrease diffusion rates through trapping lattice sites and their migration to static self-interstitials. Vacancy and site interstitial clusters annihilating one another inhibits radiation damage. The positivity of VFEs determines the stability of an alloying element which elucidates segregation [15]. Studies use simulations to investigate vacancies and their effects, and VFEs help describe these effects.

VFE is what it sounds like, the energy to form a vacancy. Vacancy energetics informs researchers about vacancy behavior. Utilizing atomistic simulation software, VFE is calculated by taking the difference between the energy of a supercell that has the vacancy and the energy of a supercell without one, in addition to the chemical potential, as discussed in the Defects section in the Introduction. This thesis will utilize implementations of LAMMPS for MD and VASP for DFT to run VFE calculations, and PYthon MATerials GENomics (pymatgen) library performed the input generation and output analysis [20].

Vacancies that require less energy to form will do so more often, and the question as to what vacancy is the most likely to form in an HEA is more complicated than when discussing other alloys. In an HEA VFE varies greatly due to the randomness of the alloy. The environment which determines the energy for vacancy formation changes not only from grain to grain, but from site to adjacent site. Therefore, to adequately evaluate vacancy formation energetics in NbMoTaW many VFE calculations need to be performed accommodating for the various possible influences on vacancy formation.

Researchers construct SQS structures anticipating many of these influences, in order to minimize the tests that are required. The VFE calculations reported for NbMoTaW in this thesis used a 128 atom SQS structure that was constructed with an algorithm implemented in the "mcsqs" code of the Alloy Theoretic Automated Toolkit (ATAT). The algorithm optimizes the shape of the supercell and the number of atomic sites so that the configurational search space for the SQS structure is not influenced by a user's specified supercell shape [21]. The structure used in this study was constructed by the authors of another study [14].

The VFEs for every atom in the SQS structure were calculated using LAMMPS initially so that a distribution of VFEs could be collected for the NbMoTaW alloy, which is similar to previous literature [15]. A plot of the computed VFEs is shown in Figure 4. Each dotted hash line separates data points into bins that designate their specie. For example, all the data points to the left of the leftmost hash line are Ta atoms, as designated by the 'Ta' lettering above that space. The data point circled in red has the lowest energies for their respective species.

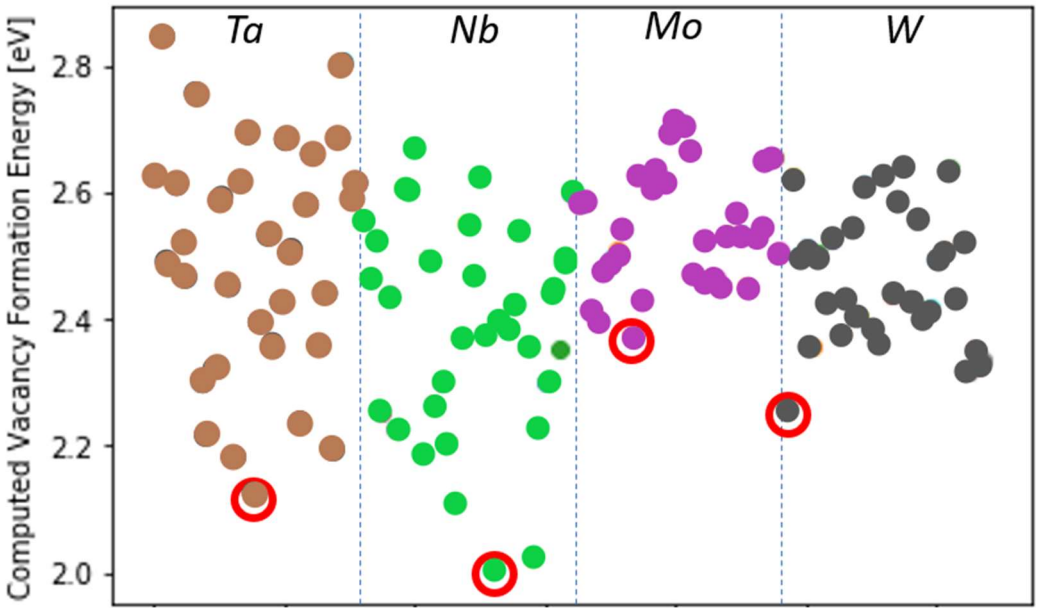

Figure 4: Computed Vacancy Formation Energies from SQS Structure in LAMMPS

As determined from Figure 4, the distribution of VFEs for Ta and Nb are far wider than Mo and W. In addition, the maximum VFE of each specie is roughly 2.7 eV while the minimum VFE ranges from 2.4 eV and 2.0 eV. This indicates Ta and Nb are more likely to form vacancies, but only under certain conditions at the atomic scale. Ta and Nb are group 5 elements and Mo and W are group 6 elements, so it is possible that the stability of group 5 elements may be more susceptible to bonding incompatibilities.

VFE calculations which utilized DFT were performed after the five smallest VFEs for each specie in the SQS structure from the LAMMPS calculations were identified. DFT was performed within the GGA using the PBE exchange-correlation functional as implemented in VASP. The simulations allowed the structure to relax when simulating the supercells with and without the vacancy. Figure 5 displays a plot of the results.

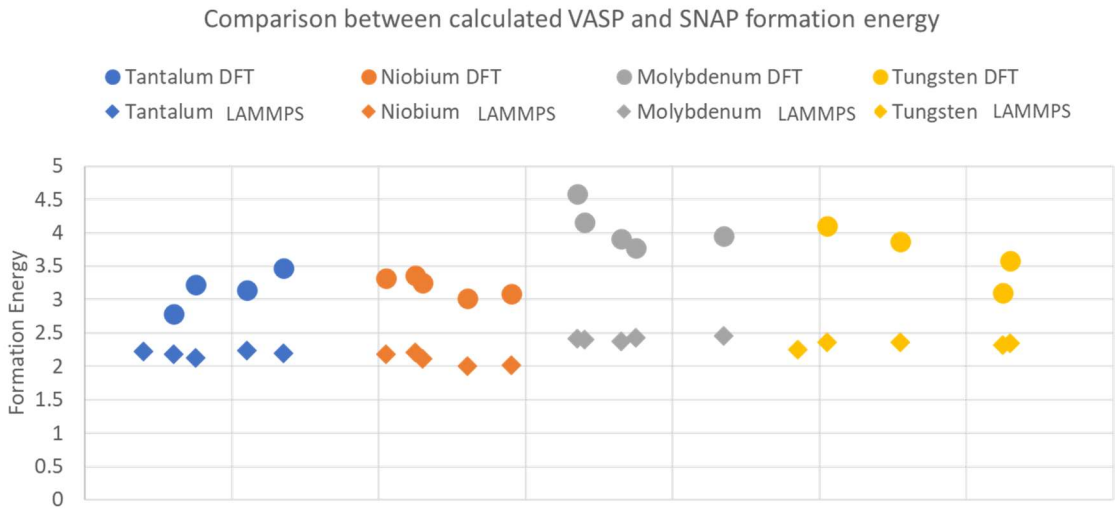

Figure 5: Computed Vacancy Formation Energies of the Five Lowest VFEs from DFT and LAMMPS for each Specie

VFEs calculated using DFT were, on average, 1.279 eV higher than LAMMPS calculations. DFT also had a wider distribution, where the standard deviation for all calculations using LAMMPS was 0.130 eV and the standard deviation for all calculations using DFT was 0.467 eV. This indicates that the effects that DFT simulates will contribute to the variability and magnitude of the VFE in NbMoTaW.

Table 1: The VFE Averages and Standard Deviations for each Specie when Using Each Simulation Software

	Ta	Nb	Mo	W
LAMMPS (Average)	2.193	2.107	2.415	2.330
DFT (Average)	3.158	3.208	4.078	3.665
LAMMPS (StDev)	0.0392	0.0827	0.0260	0.0394
DFT (StDev)	0.248	0.134	0.279	0.374

Table 1 shows data for each specie. The standard deviation of VFEs for W vacancies is an order of magnitude more when simulating with DFT instead of LAMMPs. Even though the variability of VFEs increases when simulating with DFT, some species are affected more by it than others. The lowest VFE changed between the different simulation methods, as the lowest average VFE using LAMMPS was Nb and for DFT Ta became the lowest average VFE. This was true for the lowest overall value for VFE as well, where the lowest LAMMPS VFE for Nb was 2.005 eV and 2.123 eV for Ta. When VFE was calculated using DFT the lowest Nb value was 3.020 eV and the lowest for Ta was 2.790 eV. This inconsistency demonstrates that general trends that are inferred from LAMMPS data may be incorrect.

Table 2: VFEs for Constituent Species from NbTaMoW in their Pure Form

	Ta	Nb	Mo	W
VFE [eV]	2.82	2.95	2.74	3.51

[22]

Table 2 shows calculated VFEs from another study [22]. The values reported in Table 2 are consistently higher than the values calculated in LAMMPS as reported in Table 1. Conversely, the values reported in Table 2 are consistently lower than the values calculated in DFT as reported in Table 1. Previous literature states that VFE values tend to be higher in HEAs relative to when each metal is pure [3]. The DFT data in this thesis is consistent with that trend, however the increase in VFE varies with specie. For example, the VFE for Mo increases by 1.338 eV from 2.74 eV as a pure metal and 4.078 eV in a HEA. Meanwhile, the VFE of W only goes up 0.155 eV from 3.51 eV as a pure metal and 3.665 in a HEA.

In conclusion the mechanics driven by vacancy formation will be driven by Ta and Nb atomic sites. These two species of atoms consistently had the lowest VFE, and so will be the most likely to form vacancies. The difference in LAMMPS and DFT is apparent, as LAMMPS does not capture the variability between different sites and species, while consistently calculating low VFEs. Literature supports the calculated DFT values, as the VFE is expected to be higher in HEAs relative to calculated VFE values from pure metals. The calculated VFE data does not suggest an unstable phase for the NbMoTaW alloy as none of the VFE values are negative in either LAMMPS nor DFT simulations, unlike what other studies have demonstrated in other HEAs [15].

Chapter 2: Calculating Migration Enthalpy in NbMoTaW

One of the most interesting properties of HEAs is sluggish diffusion. This is particularly true of BCC refractory HEAs like NbMoTaW as they consistently demonstrate a high thermal stability. Experimental tests showed that NbMoTaW had a stable phase at high temperatures [1] and exhibited high compressive strengths when tested with nano pillars [19]. In engineering applications, thermal stability is often a crucial aspect of materials selection. For example, turbine blades' heat tolerance limits the efficacy of an entire turbine assembly. The efficiency of power generation in turbines tends to increase as the temperature of the media of heat transfer into the turbine increases. However, with the application of high temperatures and regular cycles of centrifugal force, the turbine blades are subject to creep and the blades will fail faster relative to a system that operates at a lower temperature. Therefore, there has been a search for a material that can be used as a turbine blade that can withstand the higher temperatures to improve turbine efficiency. Ceramics have been used as turbines and see the desired high thermal efficiency. However, HEAs have superior fracture toughness to ceramics and, if the capability to manufacture them in bulk comes to pass, the World could become a safer, more energy efficient place.

Sluggish diffusion improves thermal stability, as low rates of diffusion prevent new phases from forming even at higher temperatures [3]. A study on determining diffusion behavior used vacancies to measure diffusion parameters in an FCC HEA CoCrFeMnNi [23]. The study identified that vacancy migration would tend to be slower in alloys with more alloying elements. This thesis intends to utilize vacancy diffusion simulations of the NbMoTaW alloy to study the effects of atomic changes at different distances.

The energetics of vacancy migration is useful to quantify vacancy behavior. The energy for a vacancy to move is the migration enthalpy. The migration enthalpy is calculated by taking the difference in the energy between the highest energy structure when an atom is diffusing and the lowest energy structure, when the atom is sitting in a stable lattice site. This energy can be calculated using simulations. Either MD or DFT can be used, and diffusion path for the atom which is switching sites with the vacancy is often identified with the NEB method, as described in the Defects section in the Introduction [3]. This thesis will use DFT with the climbing image NEB method. The climbing image NEB method is able to not only identify the saddle point of the diffusion path, but will increase the density of images near that saddle point, improving the calculation's accuracy [24]. The calculations for migration enthalpy were modeled after the simulations performed in a paper that constructed a high-throughput diffusion database [25].

A challenge when simulating vacancy diffusion HEAs is the same as when simulating vacancy formation in HEAs; the randomness of the alloy creates many possible influences in atomistic behavior. The strategy in this thesis for simulating the randomness NbMoTaW is by using a set of ordered structures as described in the Simulations section in the Introduction. In order to perform this test, a sufficient supercell size needs to be determined. Atomistic simulations like DFT and MD simulate a cell of atoms to predict atomic phenomena. In this thesis these cells are treated as repeating cells in all three directions. A supercell is a simulated cell of atoms that are unit cells placed next to one another. For example, a 3x3x3 supercell for a Nb structure is 27 unit cells of Nb arranged in a cube. Supercell size can influence a simulation if the phenomena being simulated causes distortion past the boundaries of the supercell. In this study, which simulates vacancy migration, a supercell size would be too small if there is strain caused by the diffusing at the edge of the cell that interacts with the stain from an adjacent cell.

These strains would amplify one another and cause an incorrect result. To determine the effective supercell sizes, migration enthalpies were calculated for the pure components of the NbMoTaW alloy, as shown in Table 3.

.

Table 3: Migration Enthalpies for Constituent Elements of NbMoTaW

Migration Enthalpy (eV) Source	Tantalum (Ta)	Niobium (Nb)	Molybdenum (Mo)	Tungsten (W)
DFT NEB calculation (3x3x3) supercell	**0.660**	**0.518**	**1.180**	**1.505**
DFT NEB calculation (4x4x4) supercell	**0.717**	**0.582**	**1.054**	**1.593**
Mattesson, et al. 2009 (exp) [26]			1.30	
Mattesson, et al. 2009 (DFT) [26]			1.30	
Schober, et al. 1992 (exp) [27]	0.7	0.55		
Mason, et al. 2017 (DFT) [28]				1.523
Schober, et al. 1992 (exp) [27]				1.7
Kittel, 2004 [29]	1.48	0.91	1.28	1.78
Ehrhart, et al. 1991 [30]	0.7-1.9	0.6-1.0	1.3-1.6	1.7-2.0
Chen, et al. 2017 (DFT) [31]			1.12	
Chen, et al. 2017 (SNAP) [31]			1.39	

The calculations in bold were performed for this thesis. They were calculated using DFT as implemented with VASP with input generated and output analyzed by pymatgen. The

calculated migration values, data in bold, are consistent with previous literature, data not shown in bold, as shown in the same Table 3. The change in supercell size has a marginal effect on the migration enthalpy, as the largest difference is 0.126 eV in Mo. This negligible change in migration enthalpies between supercell sizes demonstrates that in pure metals the simulation was large enough to accurately simulate vacancy migration.

The next step in complexity is to simulate a binary alloy with Nb and W as alloying elements. These elements were chosen in order to simulate segregation behavior due to Nb having a low VFE and W having a high VFE. Nb and W also had a lower variability so it would be easier to interpret simulation data to draw conclusions about diffusion behavior instead of less predictable interatomic forces.

To focus the simulations further, special attention will be given to the atoms closest to the diffusion path. The atoms closer to the diffusion path will have the largest influence on the energetics of the environment, so the configuration and composition of these atoms will be tweaked and adjusted. By studying a spectrum of configurations and compositions around the diffusion path, patterns about diffusion behavior in the Nb-W alloy can be interpreted. In BCC alloys, the closest vacancy diffusion path, which is the most likely, is in the [111] direction. Other diffusion directions have been simulated in previous literature, however they are uncommon [25], and so they are ignored here. There are six atoms closest to the middle of the diffusion path for BCC metals, as shown in Figure 6 visualized with VESTA. The cluster highlighted in yellow is the diffusion path and the grey atoms are the closest atoms to the midpoint of the diffusion path. In this thesis, these six atoms will be called the ‘bottleneck.’ Also, in this thesis, the set of atoms that are not being adjusted like the bottleneck atoms nor the diffusing atom will be referred to as the ‘matrix.’

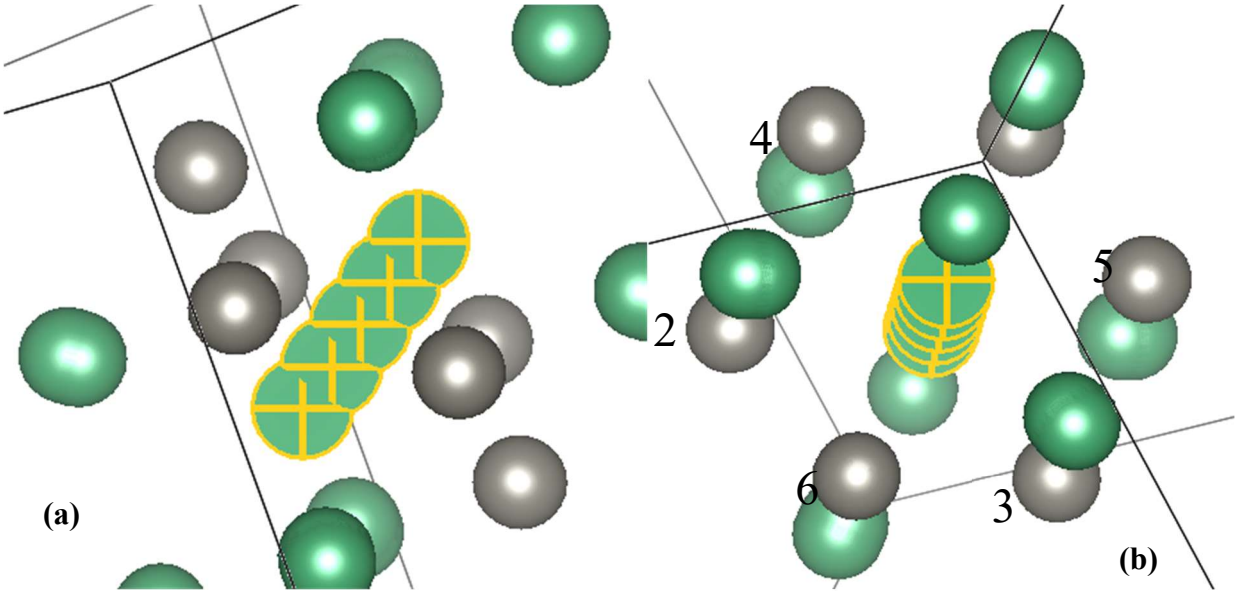

Figure 6: Profile View of Diffusion Bottleneck (a) and Top-Down View of Diffusion Path Bottleneck (b)

There are twelve unique configurations for the bottleneck to take as shown in Figure 6 if the alloy is binary. Migration enthalpies were calculated for each of these unique configurations as shown in Table 4, where a Nb atom is diffusing. The simulations allowed the structures to relax. The simulations, in addition to running simulations on each bottleneck configuration, used three different matrices, pure Nb, pure W, and a randomly generated HEA matrix which was not altered for different bottleneck configurations. The numbers in the dark blue rows correspond to the sites denoted in Figure 6 (a) and apply to the three migration enthalpy values below in the table. The numbers which refer to the sites in Figure 6 (b) signal that the site is filled with a W atom. Otherwise, a Nb atom fills the site. The same data is visualized in a bar graph in Figure 7. The simulations demonstrated a general trend where the migration enthalpy decreased as the bottleneck became more W-rich. The W matrix produced the highest migration enthalpies out of

the three matrices. From this test, it is evident that vacancy migration is affected greatly by atoms beyond the bottleneck.

Table 4: Migration Enthalpies for Nb-W Alloy for all Bottleneck Configurations and Three Matrices

W Sites	None	1	1,3	1,5	1,6	1,3,5
Nb Matrix Migration Enthalpy [eV]	0.517	0.513	0.502	0.505	0.509	0.489
W Matrix Migration Enthalpy [eV]	1.923	1.772	1.616	1.585	1.589	1.438
HEA Matrix Migration Enthalpy [eV]	1.109	1.029	0.954	0.933	0.939	0.852
W Sites	**1,5,6**	**1,3,5,6**	**1,2,5,6**	**1,2,3,5**	**1,2,3,5,6**	**1,2,3,4,5,6**
Nb Matrix Migration Enthalpy [eV]	0.477	0.466	0.464	0.471	0.455	0.447
W Matrix Migration Enthalpy [eV]	1.441	1.311	1.337	1.319	1.241	1.142
HEA Matrix Migration Enthalpy [eV]	0.848	0.769	0.753	0.769	0.684	0.621

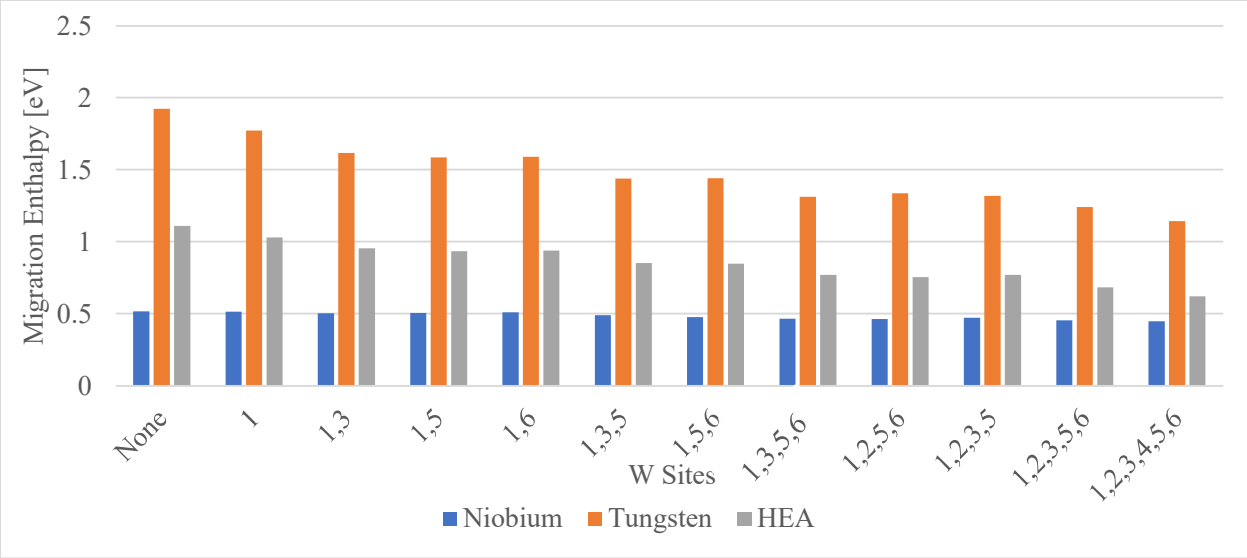

Figure 7: Bar Graph for Migration Enthalpies for Nb-W Alloy for all Bottleneck Configurations and Three Matrices (denoted in different colors)

The atomic structures included in this bottleneck study had a limited set of atomic sites that were all equidistant from the diffusion path. To better predict the effect atomic changes at different distances have on diffusion, another set of simulations was conducted. The aim of these simulations was to test diffusion on supercells where the species is changed on a larger set of atoms. Due to the larger set of atoms that were subject to changing species, the possible combinations of atomic structures to simulate would be excessive so groups of sites were changed instead. The simulated structures were adjusted such that the positions on the diffusion path that would determine the bottleneck would not only be the midpoint on the diffusion path but also the endpoints. This can be visualized in Figure 8. The endpoints are marked as red and the sites to be changed are grey. The connections between the red and grey atoms are equivalent, and include the bottleneck shown in Figure 6. The grey sites are the closest sites to the red sites, and so the grey sites are first nearest neighbors (1NN) to the red sites. In this thesis, when describing a set of sites using both endpoints and the midpoint as is shown in Figure 8, that set of

sites will be called a core. The core in Figure 8 is called the 1NN core, as the grey sites are the very closest sites to the red sites. If the core included the atoms that were the closest and the atoms that were the second closest, the set of sites would be described as second nearest neighbors (2NN). That pattern continues. This test is set up as a convergence test. The pure Nb migration enthalpy is compared to the structures with gradually increasing cores and supercell sizes. If the migration enthalpy of the pure Nb cell is similar to the migration enthalpy a structure with a core, then core has become large enough that the matrix no longer has an effect on diffusion. If the matrix no longer has an effect, it is negligible, and less atomic configurations need to be tested.

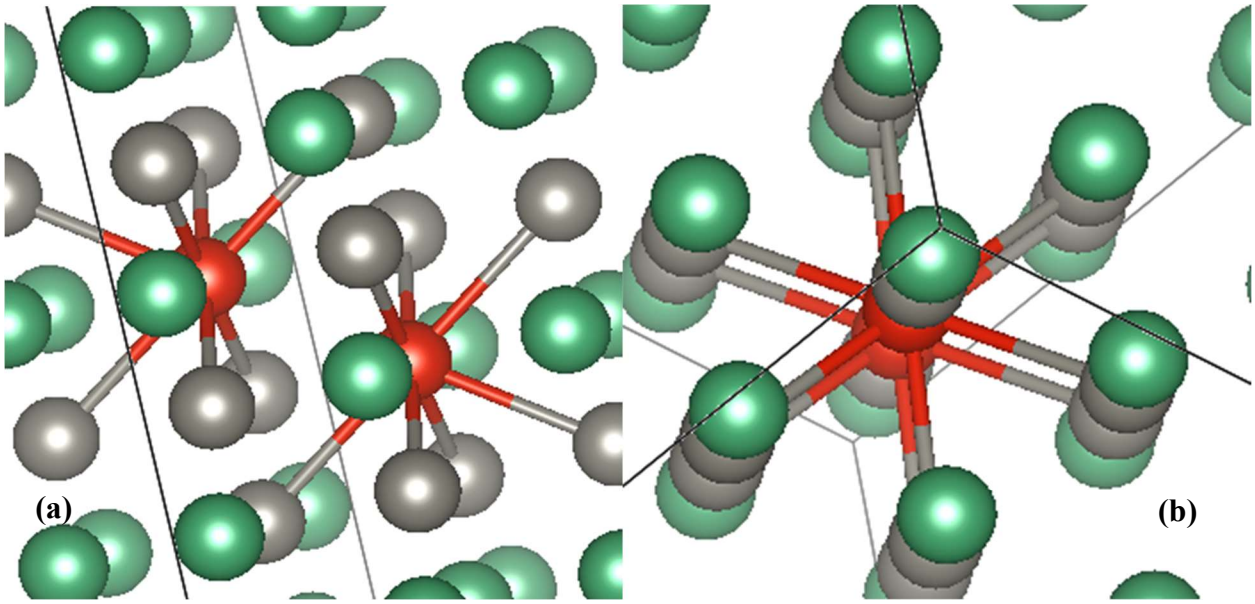

Figure 8: Profile View of 1NN Core (a) and Top-Down View of 1NN Core (b)

The results of the simulations comparing core sizes are shown in Table 5 and Table 6. These simulations all had W matrices and Nb was the diffusing atom. The range of super cells went from 3x3x3 to 5x5x5 and the core size ranged from 1NN to 5NN. The calculations used

either relaxed or fixed cells. The relaxed cells are simulations that allowed the lattice parameter of the material to relax at an equilibrium. Fixed cells are simulations that required the lattice parameter to be the same as W, which is larger than Nb. Graphical representations of both tables are shown in Figure 9 and Figure 10.

Table 5: Relaxed Cell Migration Enthalpy [eV] Calculations with Different Core Sizes

Super Cell Size	Pure Nb	W Matrix 1NN Nb	W Matrix 2NN Nb	W Matrix 3NN Nb	W Matrix 4NN Nb	W Matrix 5NN Nb
3x3x3	0.530	1.308	1.212	0.919	0.787	0.782
4x4x4	0.489	0.902	1.014	1.308	1.123	0.994
5x5x5	0.490	1.109	1.110	1.356	0.951	0.848

Table 6: Fixed Cell Migration Enthalpy [eV] Calculations with Different Core Sizes

Super Cell Size	Pure Nb	W Matrix 1NN Nb	W Matrix 2NN Nb	W Matrix 3NN Nb	W Matrix 4NN Nb	W Matrix 5NN Nb
3x3x3	0.530	1.234	1.078	0.770	0.779	0.776
4x4x4	0.489	0.751	0.837	1.152	1.021	0.924
5x5x5	0.490	0.875	0.940	1.221	0.882	0.805

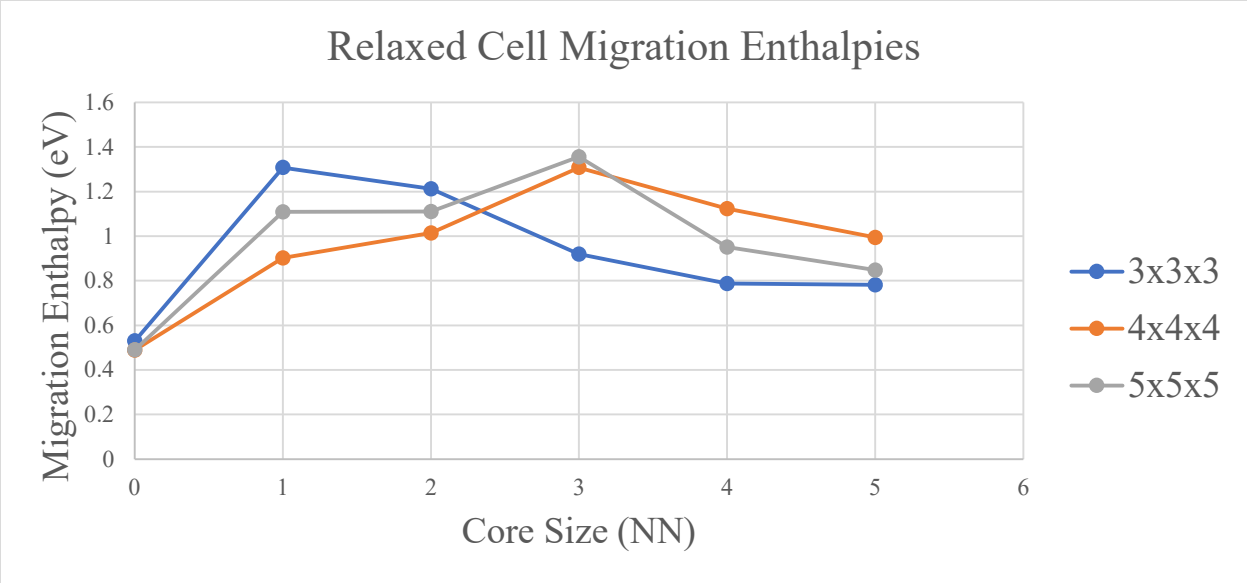

Figure 9: Graph of Relaxed Cell Migration Enthalpies with Different Core Sizes

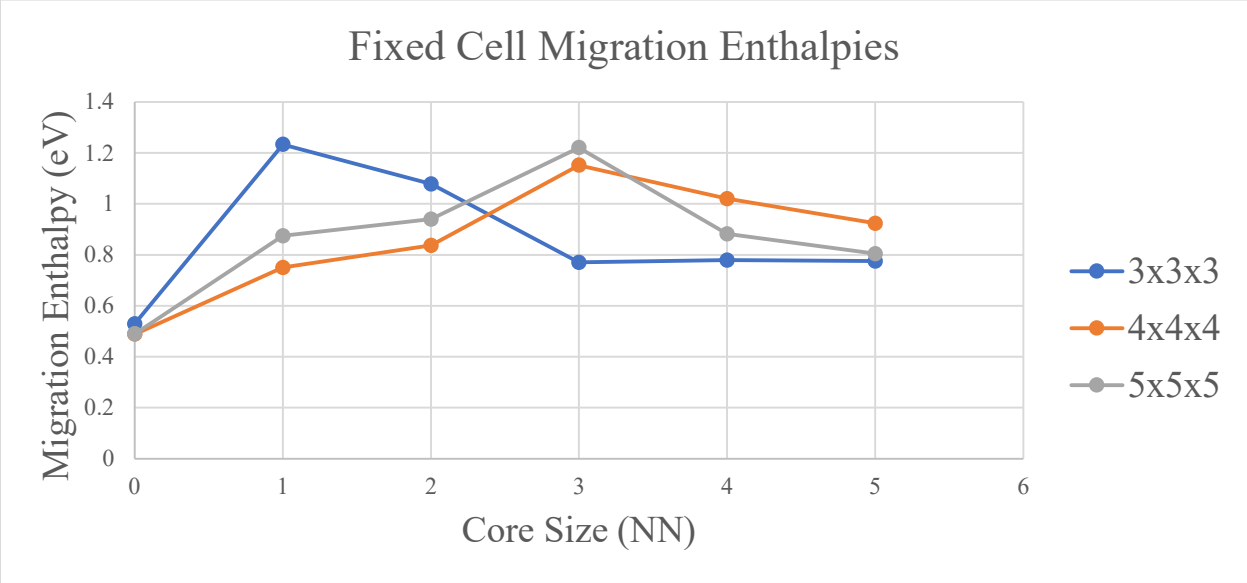

Figure 10: Graph of Relaxed Cell Migration Enthalpies with Different Core Sizes

The bottleneck study demonstrated how significantly diffusion can be affected by the adjacent atoms and the atoms in the matrix. As shown in Table 4 the specie of the bottleneck could change the migration enthalpy by up to 0.781 eV and the atoms that filled the matrix changed the migration enthalpy significantly. The average migration enthalpy for the Nb matrix

in the bottleneck test was 0.485 eV, 1.476 eV for the W matrix, and 0.855 eV for the HEA matrix. These trends for the migration enthalpies agreed with prior literature as the migration enthalpy in the HEA matrix were in the same order of magnitude as the pure metals [3]. It is possible that more tests with an HEA bottleneck would have a more significant effect.

The core study used a consistent matrix and core specie, however different core sizes were simulated. Performing these simulations helped predict the distance at which atomic changes will not affect diffusion behavior. This was done by comparing pure Nb supercells with supercells that have W matrices with Nb cores. If the Nb core becomes large enough, the migration behavior should be similar to pure Nb supercells. Observing Figure 9 and Figure 10, this was not reached within a 5x5x5 supercell with a 5NN core, which had a migration enthalpy 0.315 eV higher than the 5x5x5 pure Nb supercell. Past a 5x5x5 supercell DFT simulations became too costly. However, after a peak migration enthalpy with a 3NN core the migration enthalpy began to stabilize with larger cores in the 4x4x4 and 5x5x5 supercells. The 3x3x3 supercell did not see this as the core was large enough to extend past the boundary of the supercell.

Chapter 3: Conclusion and Future Work

The study on simulating vacancy behavior found that the calculated VFE data agreed with previous literature. DFT simulations demonstrated higher VFEs in the HEA relative to the constituent alloying elements in pure metals. This finding is consistent with previous literature in that the higher VFE values will retard diffusion rates. These results demonstrate that the HEAs will inhibit vacancy formation. DFT simulations predicted VFEs that were not only higher in magnitude but also varied far more than MD calculations as shown in Figure 5. The error in the MD simulations showed that complexities in the bonding characteristics in the HEA were ignored. MD simulations would need ML techniques, like SNAP or GAP, to fill that discrepancy.

The relationship between the migration enthalpy and changing the bottleneck configuration was more tied with atomic composition than any particular pattern. Changing the matrix had the most significant effect on migration enthalpies. The Nb matrix produced the lowest migration enthalpies, W the highest, and the HEA was in between, which agreed with previous literature. The core studies showed how sensitive diffusion is to atomic changes in the NbMoTaW alloy. Migration enthalpies never returned to the same value as the pure Nb structures, however they began to plateau after the 3NN core. This made the error associated with the matrix of the structure to be more predictable and therefore is sufficient for testing HEAs. It also elucidates the migration enthalpy's sensitivity to atomic changes even far away from the diffusion path.

The next step would be to apply ML methods and expand these studies. SNAP can be used, as it has been in investigating other segregation behavior in NbMoTaW [14], to improve

MD simulations for VFE calculations. The studies on diffusion can be combined by calculating migration enthalpies for different combinations of atoms in the core to better predict HEA behavior. This thesis showed that the matrix could be corrected for and so that decreases the amount of simulations that need to be performed. Atomic configurations could be identified that either inhibit or facilitate it. Trapping sites would be an interesting atomic configuration to simulate and compare to other structures.

References

[1] X. Feng, J. Zhang, Z. Xia, W. Fu, K. Wu, G. Liu, and J. Sun, "Stable nanocrystalline NbMoTaW high entropy alloy thin films with excellent mechanical and electrical properties," *Mater. Lett.*, vol. 210, no. 1, pp. 84–87, Jan. 2018, doi: 10.1016/j.matlent.2017.08.129.

[2] M. Zheng, W. Ding, W. Cao, S. Hu, and Q. Huang, "A quick screening approach for design of multi-principal element alloy with solid solution phase," *Mater. Des.*, vol. 179, p. 107882, Oct. 2019, doi: 10.1016/j.matdes.2019.107882.

[3] Z. H. Aitken, V. Sorkin, and Y.-W. Zhang, "Atomistic modelling of nanoscale plasticity in high-entropy alloys," *J. Mater. Res.*, pp. 1–24, Jan. 2019, doi: 10.1557/jmr.2019.50.

[4] Z. Fu, W. Chen, H. Wen, D. Zhang, Z. Chen, B. Zheng, and E. J. Lavernia, "Microstructure and strengthening mechanisms in an FCC structuredsingle-phase nanocrystalline Co25Ni25Fe25Al7.5Cu17.5high-entropyalloy," *Acta Mater.*, vol. 107, pp. 59–71, 2016.

[5] X. B. Feng, J. Y. Zhang, Y. Q. Wang, Z. Q. Hou, K. Wu, G. Liu, and J. Sun, "Size effects on the mechanical properties of nanocrystalline," *Int. J. Plast.*, pp. 1–25, 2017, doi: 10.1016/j.ijplas.2017.04.013.

[6] O. N. Senkov, D. B. Miracle, and K. J. Chaput, "Development and exploration of refractory high entropy alloys-A review," *J. Mater. Res.*, vol. 33, no. 19, pp. 3092–3128, Oct. 2018, doi: 10.1557/jmr.2018.153.

[7] S. Lee, M. J. Duarte, M. Feuerbacher, R. Soler, C. Kirchlechner, C. H. Liebscher, and G. Dehm, "Dislocation Plasticity in FeCoCrMnNi high-entropy alloy: quantitative insights from in situ transmission electron microscopy deformation," *Mater. Res. Lett.*, vol. 8, no. 6, pp. 216–224, 2020, doi: 10.1080/21663831.2020.1741469.

[8] D. S. Sholl and J. A. Steckel, "Density functional theory, a practical introduction," in *Density functional theory, a practical introduction*, D. S. Sholl and J. A. Steckel, Eds. Hoboken: John Wiley & Sons, Inc, 2009, p. 11.

[9] P. M. Chaikin and T. C. Lubensky, "Principles of condensed matter physics," in *Principles of condensed matter physics*, P. M. Chaikin and T. C. Lubensky, Eds. Cambridge: Cambridge University Press, 1995, pp. 144–212.

[10] Y. H. Zhang, A. H. Zhuang, J. J. Kai, and C. T. Liu, "The origin of negative stacking fault energies and nano-twin formation in," *Scr. Mater.*, pp. 96–99, 2016, doi: 10.1016/j.scriptamat.2016.11.014.

[11] Y. Wang, M. Yan, Q. Zhu, W. Y. Wang, Y. Wu, X. Hui, and L.-Q. Chen, "Computation of entropies and phase equilibria in refractory," *Acta Mater.*, pp. 88–101, 2018, doi: 10.1016/j.actamat.2017.10.017.

[12] W.-M. Choi, Y. H. Jo, S. S. Sohn, S. Lee, and B.-J. Lee, "Understanding the physical metallurgy of the CoCrFeMnNi," *Comput. Mater.*, pp. 1–9, 2018, doi: 10.1038/s41524-017-0060-9.

[13] J. Behler and M. Parrinello, "Generalized neural-network representation of high-dimensional potential energy surfaces," *Phys. Rev. Lett.*, vol. 146401, pp. 1–4, 2007, doi: 10.1103/PhysRevLett.98.146401.

[14] X.-G. Li, C. Chen, H. Zheng, Y. Zuo, and S. P. Ong, "Complex strengthening mechanisms in the NbMoTaW multiprincipal," *Comput. Mater.*, pp. 1–10, 2020, doi: 10.1038/s41524-020-0339-0.

[15] S. C. Middleburgh, D. M. King, G. R. Lumpkin, M. Cortie, and L. Edwards, "Segregation and migration of species in the CrCoFeNi high entropy alloy," *J. Alloys Compd.*, vol. 599, pp. 179–182, Jun. 2014, doi: 10.1016/j.jallcom.2014.01.135.

[16] M. Vaidya, T. Simon, B. S. Murty, G. Wilde, and Divinski, "Ni tracer diffusion in CoCrFeNi and CoCrFeMnNi high entropy alloys," *J. Alloys Compd.*, vol. 688, pp. 994–1001, 2016, doi: 10.1016/j.jallcom.2016.07.239.

[17] Z. Wang, C. T. Liu, and P. Dou, "Thermodynamics of vacancies and clusters in high-entropy alloys," *Phys. Rev. Mater.*, vol. 1, no. 043601, pp. 1–5, 2017, doi: 10.1103/PhysRevMaterials.1.043601.

[18] S. L. Thomas and S. Patala, "Vacancy diffusion in multi-principal element alloys: the role of chemical disorder in the ordered lattice," *Acta Mater.*, pp. 144–153, 2020, doi: 10.1016/j.actamat.2020.06.022.

[19] S. Zhao, T. Egami, G. M. Stocks, and Y. Zhang, "Effect of d electrons on defect properties in equiatomic NiCoCr and NiCoFeCr," *Phys. Rev. Mater.*, vol. 2, no. 013602, pp. 1–8, 2018, doi: 10.1103/PhysRevMaterials.2.013602.

[20] S. P. Ong, W. D. Richards, A. Jain, G. Hautier, M. Kocher, S. Cholia, and G. Ceder, "Python materials genomics (pymatgen) : A robust, open-source python library for materials analysis," *Comput. Mater. Sci.*, pp. 314–319, 2013, doi: 10.1016/j.commatsci.2012.10.028.

[21] A. Walle, P. Tiwary, M. Jong, D. L. Olmsted, M. Asta, A. Dick, and L.-Q. L.-K. Chen, "Efficient stochastic generation of special quasirandom structures," *CALPHAD Comput. Coupling Phase Diagr. Thermochem.*, vol. 42, pp. 13–18, 2013, doi: 10.1016/j.calphad.2013.06.006.

[22] B. Medasani, M. Haranczyk, A. Canning, and M. Asta, "Vacancy formation energies in metals: A comparison of MetaGGA," *Comput. Mater. Sci.*, vol. 101, pp. 96–107, 2015, doi: 10.1016/j.commatsci.2015.01.018.

[23] K.-Y. Tsai, M.-H. Tsai, and J.-W. Yeh, “Sluggish diffusion in Co–Cr–Fe–Mn–Ni high-entropy alloys,” *Acta Mater.*, vol. 61, pp. 4887–4897, 2013, doi: 10.1016/j.actamat.2013.04.058.

[24] G. Henkelman, B. Uberuaga, and Jónsson, “A climbing image nudged elastic band method for finding saddle points and,” *J. Chem. Phys.*, vol. 113, pp. 9901–9904, 2000, doi: 10.1063/1.1329672.

[25] H. Wu, T. Mayeshiba, and D. Morgan, “High-throughput ab-initio dilute solute diffusion database,” *Sci. Data*, vol. 3, no. 160054, pp. 1–7, 2016.

[26] T. R. Mattsson, N. Sandberg, R. Armiento, and M. A. E, “Quantifying the anomalous self-diffusion in molybdenum with first-principles simulations,” *Phys. Rev. B Condens. Matter Mater. Phys.*, vol. 80, no. 22, p. 224104, 2009.

[27] H. R. Schober, W. Petry, and J. Trampenau, “Migration enthalpies in FCC and BCC metals,” *J. Phys. Condens. Matter*, vol. 4, pp. 9321–9338, 1992, doi: 10.1088/0953-8984/4/47/013/pdf.

[28] D. R. Mason, D. Nguyen-Manh, and C. S. Becquart, “An empirical potential for simulating vacancy clusters in tungsten,” *J. Phys. Condens. Matter*, vol. 29, no. 50, p. 505501, Nov. 2017, doi: 10.1088/1361-648X/aa9776.

[29] C. Kittel, *Introduction to solid state physics*, 8th ed. Hoboken: Wiley, 2004.

[30] P. Ehrhart and H. Ullmaier, *Atomic defects in metals*. Berlin: Springer-Verlag, 1991.

[31] C. Chen, Z. Deng, R. Tran, H. Tang, I.-H. Chu, and S. P. Ong, “Accurate force field for molybdenum by machine learning,” *Phys. Rev. Mater.*, vol. 1, no. 4, pp. 1–25, 2017, doi: 10.1103/PhysRevMaterials.1.043603.